energies

MDPI

Article

Analysis of an Urban Grid with High Photovoltaic and e-Mobility Penetration

Florian Maurer *, Christian Rieke, Ralf Schemm and Dominik Stollenwerk

FH Aachen—NOWUM-Energy, University of Applied Sciences Aachen, 52428 Jülich, Germany; rieke@fh-aachen.de (C.R.); schemm@fh-aachen.de (R.S.); stollenwerk@fh-aachen.de (D.S.)
* Correspondence: maurer@fh-aachen.de; Tel.: +49-241-6009-54265

Abstract: This study analyses the expected utilization of an urban distribution grid under high penetration of photovoltaic and e-mobility with charging infrastructure on a residential level. The grid utilization and the corresponding power flow are evaluated, while varying the control strategies and photovoltaic installed capacity in different scenarios. Four scenarios are used to analyze the impact of e-mobility. The individual mobility demand is modelled based on the largest German studies on mobility "Mobilität in Deutschland", which is carried out every 5 years. To estimate the ramp-up of photovoltaic generation, a potential analysis of the roof surfaces in the supply area is carried out via an evaluation of an open solar potential study. The photovoltaic feed-in time series is derived individually for each installed system in a resolution of 15 min. The residential consumption is estimated using historical smart meter data, which are collected in London between 2012 and 2014. For a realistic charging demand, each residential household decides daily on the state of charge if their vehicle requires to be charged. The resulting charging time series depends on the underlying behavior scenario. Market prices and mobility demand are therefore used as scenario input parameters for a utility function based on the current state of charge to model individual behavior. The aggregated electricity demand is the starting point of the power flow calculation. The evaluation is carried out for an urban region with approximately 3100 residents. The analysis shows that increased penetration of photovoltaics combined with a flexible and adaptive charging strategy can maximize PV usage and reduce the need for congestion-related intervention by the grid operator by reducing the amount of kWh charged from the grid by 30% which reduces the average price of a charged kWh by 35% to 14 ct/kWh from 21.8 ct/kWh without PV optimization. The resulting grid congestions are managed by implementing an intelligent price or control signal. The analysis took place using data from a real German grid with 10 subgrids. The entire software can be adapted for the analysis of different distribution grids and is publicly available as an open-source software library on GitHub.

Keywords: e-mobility; smart-charging; distribution grid simulation

Citation: Maurer, F.; Rieke, C.; Schemm, R.; Stollenwerk, D. Analysis of an Urban Grid with High Photovoltaic and e-Mobility Penetration. *Energies* **2023**, *16*, 3380. https://doi.org/10.3390/en16083380

Academic Editors: Evangelos Karfopoulos, Michele Roccotelli and Ioannis Karakitsios

Received: 13 February 2023
Revised: 29 March 2023
Accepted: 4 April 2023
Published: 12 April 2023

1. Introduction

The German government has set itself the goal of reducing greenhouse gas emissions in the transport sector by 48% by 2030 compared with 1990. This requires the electrification of transport and the use of renewable energies. A prerequisite for this is the further expansion of the charging infrastructure. The transformation from fossil energy to renewable energy sources (RES) started in the year 2004 by setting the first novel of the "Erneuerbaren-Energien-Gesetz" (EEG—Law) in charge to meet the EU climate objectives. In 2020, the average yearly share of the electric energy generated by renewables in Germany was 45% [1].

Due to the time-dependent availability of RES and further decentralization of the electricity generation, the power system is changing. On the other hand, the expanding market of Electric Vehicles (EVs) is an additional challenge, which creates a lot of decentralized demand and provides an interesting potential as storage. The German objective of one

million EVs on the roads by 2020 was not achieved, but current developments and forecasts indicate a successful ramp-up. In 2020, about 200,000 funding applications are submitted for EVs, and 360,000 EVs were subsidized in 2021 [2]. By 2030, the German government aims for seven to ten million EVs, while the German Association of the Automotive Industry expects 10.5 million EVs [3].

To meet this objective, capable charging infrastructure and control of this infrastructure is required. It is planned to increase the amount of available public charging stations from 21,000 in 2021 to one million in 2030. This plan corresponds with the EU's objective of a ratio of EVs to public charging points of 10:1 [4]. Additionally, 7.1 million charging points in private households are required to ensure the electrification of the transport sector [5]. The share of private charging operations is estimated up to 88%, which results in additional consumption of 10,000 GWh in the low voltage grids, especially in urban regions. In the public domain, 12% of charging operations will be carried out with a corresponding energy volume of 12,000 GWh in 2030 [5].

As grid planning allocates resources for decades of operation, large parts of today's distribution grids were not planned for today's demand of electrification. Multiple studies show that simultaneous charging during peak hours can exhaust and exceed the current grid capacities [6–10].

To avoid congestion, either a grid reinforcement or an intelligent control system can be applied. Therefore, time-dependent charging prices are already considered and tested in some areas [11]. Different simulation tools can model energy system expansion and investments on a larger scale [12], while this study investigates whether congestion in the distribution grid can be reduced with the help of simple controlling or dynamic prices. Individual charging behavior is rarely investigated thoroughly, resulting in high assumptions about concurrent charging processes.

2. Related Work

Distribution grids and possible control signals for EVs have been investigated in many previous studies. The approaches to mapping mobility behavior, the charging strategies, and the modelling approach for the energy supply units and the energy distribution grids vary considerably between the individual studies.

In this section, some studies related to modelling of price-sensitive charging behavior are cited, and their strategies are compared to the ones developed in this paper. The research in this field is conducted worldwide and evolves dynamically, and therefore, the related work is multifaceted. The adapted approaches before the year 2015 are summarized in Gottwalts PhD thesis [13], where he found that Time-of-Use-based pricing can be used to achieve demand response for small shares of flexible loads and investigates group-based pricing in contrast to Realtime pricing. Growing databases and a partial mapping of user behavior were the basis for subsequent works in particular, summarized by Su in the year 2020 [14]. He updates the existing knowledge basis and gives a broad overview of existing EV models, charging strategies and ToU-based vs. group-based pricing approaches for demand response. A high potential for load-shifting EV charging was found in [15], as constantly about 45% of cars are available. However, the most recent studies consider latest EV models, their charging behavior, and the resulting demand response to price signals with different approaches in [16–25]. In [16,17], the EV demand is modeled deterministically considering a non-sensitive approach, such as the first charging strategy *Base Case* chosen in this paper. The first modelling approach presented in this paper is a more flexible adaptive approach with a fixed cap, represented by a maximum willingness to pay for the energy. In the result, the EV users only charge if the SoC is below the required SoC of the coming day. Furthermore, we have derived individual functions of willingness to pay depending on the state of charge based on surveys to further refine the charging strategy.

Many approaches generate scenario data through sampling from existing data to create scenarios with future higher charging demand as seen in [20–22]. A total of 29,262 existing EV charging curves were used in [22] to sample the power demand. A specific

case comparing uncontrolled and controlled charging is shown in [26,27], while the economic investment and operation cost were considered in [28].

Yet those approaches do not model price sensitivity and the responding displacement of charging demand. Such factors can be determined by using a stochastic probabilistic simulation with consideration of the grid aspects [18,29–31]. A similar approach to investigate grid planning was done in [32], which investigates four different charging station location cases. The authors in [23] propose a probability-based approach and compare price sensitive and non-sensitive demands with the result of much lower maximum demand and a shift toward the evening hours from 7 and 10 am without sensitivity.

The investigation of PV potentials in the context of E-Mobility was done in [33], where different PV and EV penetration cases were modelled using three different charging behaviors without price sensitivity in a cell-based grid model.

In [24], the EV charging demand is controlled in an indirect manner by adopting a dynamic virtual pricing mechanism according to the forecasted EV charging demand and local renewable generation production. The objective of the EV Agents is to minimize their individual charging cost, according to the price values and therefore schedule the charges at the cheapest hours. This modelling approach is very similar to the second *Case B* and *Case C* charging strategy presented in this paper where the maximization of the PV consumption in the individual households and the maximization of a user satisfying function determine the charging schedule for the EVs. The main difference to the approaches in this paper are the usage of real distribution grid data, PV integration, and energy consumption data for this grid and the benefit function usage as optimization objective.

3. Materials and Methods

In this section, the methods that are used to model the mobility behavior, the resulting charging demand, and the ordinary power demand are explained. In addition, the applied dynamic grid fee and the different scenario cases are derived.

The overall agent-based simulation framework is implemented in Python with common libraries such as *NumPy*, *Pandas* and *GeoPandas*, *PyPSA* and *PVLib*. The results are stored using the timeseries database *TimescaleDB* and are evaluated with the help of a geo referenced data store extension *PostGIS*. To orchestrate the multiple simulation runs across a cluster of HPC servers, the technology *Docker Swarm* is used. Yet, single simulations can also be run on a consumer laptop. To solve the optimization, any solver supported by the solver library pyomo can be used, for example *GLPK*.

3.1. Simulation Framework & Sequence

The framework is designed in such a way that several scenarios/simulations can be calculated in parallel. For this purpose, each simulation is started in a separate Docker container. The containers work on the same database, so that the results can be easily summarized and analyzed.

The scenarios differ depending on the considered user behavior. In the *Base Case*, the user requests a charging process after his journey. A request is always made if the current SoC of the vehicle is not sufficient for the mobility needs of the next day. For example, if the vehicle only has 15% left after the journey, but 45% is needed for the next day, the consumer sends a request to fully charge his EV to 100%. In this case, the charging process is planned so that it starts at the next time step t and continues until the vehicle is fully charged at his nominal power P_{car}.

Depending on the level of the dynamic grid fee G_t, the charging process is accepted and carried out or suspended. If the price level is too high, charging is suspended for 30 min until the user makes another request. A maximum of five rejections are possible until the consumer commits even at higher costs.

This corresponds to the assumption that the need for mobility is always more worth as the total cost of charging, and that the consumer accepts this cost to reach his workplace

the next day, for example. The following steps and the corresponding Figure 1 summarize the simulation process in detail for the *Base Case*.

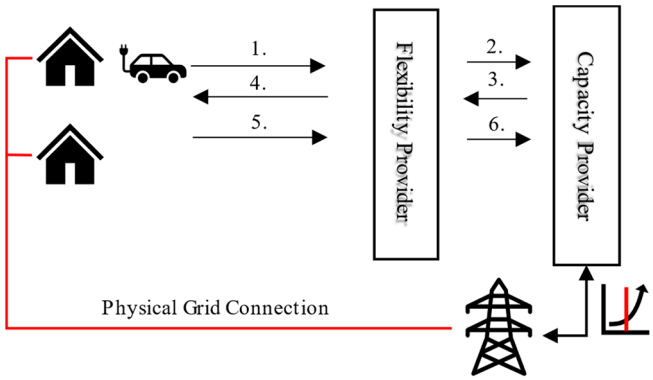

Figure 1. Simulation sequence of the developed simulation framework SmartDSO. The figure shows general simulation steps (1–6) and price communication between price-sensitive mobility demand and the grid fees depending on congestion calculated by the capacity provider.

1. The Consumer sends a charging request for the next simulation period (15 min)
2. The Flexibility Provider maps the demand on the corresponding grid node and sends demand to the Capacity Provider.
3. The Capacity Provider calculates the total grid utilization and answers with a grid fee time series.
4. The Flexibility Provider communicates the Price Level to the Consumer.
5. The Consumer can lock the demand to the current price level and sends a commit or reject message back.
6. Corresponding to the answer, the Flexibility Provider send final demand time series to the Capacity Provider.

In the other scenarios (*Case A*, *Case B*, and *Case C*), each consumer solves an optimization problem at the beginning of each day. Input variables of the optimization are the PV generation and the consumption, resulting from a Standard Load Profile (SLP). The journeys of the day are also considered, as well as the required SoC of the coming day. At the end of the day, the SoC must fulfil the same requirement that is also used in the *Base Case*. In addition, the electricity tariff of the end consumer, including surcharges and taxes, as well as the dynamic grid fee are considered. The grid fee is initially assumed to be 2.5 ct/kWh for the first calculation of the five possible optimization runs.

The Capacity Provider receives a request for the next 96 quarter hours from all consumers who want to charge their EV via the electricity grid. The capacity provider processes the requests in the order in which they were made. Only when the six steps from Figure 1 have been processed for a consumer, the next consumer is handled.

If a consumer rejects the request because, for example, the grid fees exceed the initial 2.5 ct/kWh, it carries out another optimization with the new grid fee information at each time step t. The result of the optimization is either a disclaimer of the recharge because the grid fee is too high in all hours, or a shift to other hours in which the grid fee is lower. The consumer always accepts the last of his five offers, even if the price is higher than the price limit. The objective function of the optimization problem can be formulated as shown in Equation (1).

$$\max\left(B - \sum_{t}^{T} PRequest_t \cdot Tarif_t\right) \tag{1}$$

The users living in a residential area want to maximize their benefit B, meaning to maximize the usage with cheapest cost. For this purpose, a utility function is used, which is defined in *Case A* and *Case B* via a linear function between SoCs of the cars and the

price limit. In the last *Case C*, the integral of the demand functions, which are derived in Section 3.3, is used. These are linearized piecewise using the following Equations (2)–(6).

$$\sum_s z_s = 1 \tag{2}$$

$$q_s \geq SegVLow_s \cdot z_s \; \forall \; s \tag{3}$$

$$q_s \leq SegVUp_s \cdot z_s \; \forall \; s \tag{4}$$

$$B = \sum_s \begin{matrix} SegBLow_s \cdot z_s + \\ SegCoeff_s \cdot (q_s - SegVLow_s \cdot z_s) \end{matrix} \tag{5}$$

$$VTotal = \sum\nolimits_s qs \tag{6}$$

The linearization is explained in detail in [34,35]. To increase the benefit B, the car must be charged. This can be done either via a photovoltaic system Ppv_t or by purchasing requested electricity $PRequest_t$ from the grid. If the benefit gain ΔB is lower than the additional cost $Tarif_t$, the car is not charged any further. The Equations (7)–(9) show the corresponding balancing of the charging power $PCharge_t$, the power of the photovoltaic system Ppv_t and the grid purchase $PRequest_t$ at time step t.

$$PRequest_t = PCharge_t - Ppv_t \tag{7}$$

$$PGen_t - Ppv \geq 0 \; \forall \; t \in T \tag{8}$$

$$PRequest_t \geq 0 \; \forall \; t \in T \tag{9}$$

The charging power $PCharge_t$ is the sum of the individual capacities for each car in the household (see Equation (10)). The car can only be charged when it is not in use and when it is at home (see Equation (11)).

$$PCharge_t = \sum\nolimits_{car}^{C} P_{car,t} \tag{10}$$

$$P_{car,t} \leq (1 - U_{car,t}) \cdot PMax_{car} \; \forall \; t \in T, \; car \in C \tag{11}$$

Finally, the SoC level of a car is restricted to the lower limit 0 and the upper limit $EMax_{car}$ as shown in Equations (12)–(14).

$$\begin{matrix} V_{car,t} = V_{car,t-1} + P_{car,t} \cdot dt - EDem_{car,t} \\ \forall \; t \in T, \; car \in C \end{matrix} \tag{12}$$

$$\begin{matrix} 0 \leq V_{car,t} \leq E_{car} \\ \forall \; t \in T, \; car \in C \end{matrix} \tag{13}$$

$$VTotal = \sum\nolimits_{car}^{C} V_{car,T} \tag{14}$$

The study examines four scenarios. For each scenario, the degree of PV expansion is varied between 25% and 100% of the potential maximum capacity in the supply area. The scenarios differ in the modelling of the charging behavior of the consumers and the used electricity tariff. In the first two cases (*Base* and *A*), the end consumers receive a fixed electricity price that corresponds to the average of the day-ahead prices for the analyzed period. In the simulation, the month of May in 2022 is examined. In *Case B* and *C*, the hourly

day-ahead price is directly passed on to the consumers. A further 10.8 ct/kWh in surpluses and taxes is added to both the fixed price and the dynamic day-ahead price. Depending on the grid utilization, a dynamic grid fee is added to every requested charging process.

In the *Base Case*, no optimization takes place regarding an objective value. Drivers always request a charging process via the Capacity Provider when they return from a journey and the SoC of their vehicle is no longer sufficient for the journey on the following day. This is described by the SoC limit $SoCLimit_t$. The Consumers have a fixed price limit of 45 ct/kWh. If the charging price is on average more expensive than the limit, the charging process is shifted in hours with less utilization.

In *Case A*, the described optimization takes place at the beginning of each day. The objective value is the maximization of electricity consumption from the own PV system. For this purpose, it is assumed that the PV generation for the coming day is already known. Thus, any uncertainty in PV generation at the time of optimization is not considered. Analogous to the *Base Case*, electricity is only consumed from the grid if the SoC is no longer sufficient for the upcoming mobility demand. Otherwise, only the use of the own PV System is possible. If the average price of a request is again above the limit of 45 ct/kWh, the charging process is shifted again.

In *Case C*, the objective value is the maximization of a benefit function *B*, which leads to a maximum PV usage and a charging at the cheapest hours. The SoC-dependent benefit function B is described in detail in Section 3.3. In *Case B*, the fixed price cap of 45 ct/kWh is applied. For each scenario case, serval simulations are calculated to get a distribution of possible grid congestions. Table 1 summarize the scenarios.

Table 1. Simulation parameters of investigated scenarios.

Scenario	Charging Strategy	Market	Grid Fee	Mobility Behavior
Base Case	SoC independent	Flat Price	dynamic	random
Case A	maximize PV usage + SoC independent	Flat Price	dynamic	random
Case B	maximize PV usage + SoC independent	Spot Price	dynamic	random
Case C	maximize PV usage + SoC dependent	Spot Price	dynamic	random

3.2. Agents in the Simulation Framework

The agent of the capacity provider calculates the grid utilization and the resulting dynamic grid fee G_t of the requested charging process. The function in Equation (15) is used to calculate the dynamic fee. The function increases monotonically until it reaches its maximum value of 100 ct/kWh at a utilization of 100%. From this limit, the price remains constant. To model the function G_t, the current grid fees in Germany were analyzed. According to [24], the average grid fee for residential areas is approximately 7.5 ct/kWh. A difference of 2.0–3.0 ct/kWh is possible. In this study, a minimum of 2.6 ct/kWh is chosen, and the common 7.5 ct/kWh at a utilization of 40%.

$$G_t = \max_{n \in N} \left(0.15 \cdot \left(0.175 - \ln \left(1 - u_{n,t}^{\frac{2}{3}} \right) \right) \right) \tag{15}$$

To calculate the grid fee G_t, the highest utilization of the component n at the respective time t in the corresponding sub-grid is used. The end consumer or the flexibility provider receives the dynamic grid fee for each requested point in time.

To determine the utilization of each grid component, a calculation of the power flow is carried out using the Python package PyPSA [35]. The power flow corresponds to the solution of a non-linear system of equations, which is solved using the Newton Raphson method. Since the capacity provider cannot directly control the charging of the EVs, the optimal power flow is not calculated, as often in other studies including [9,36]. Therefore, the capacity provider does not solve an optimization task by dispatching the demand and generation, but the dispatch of the consumers takes place via the dynamic grid fee.

In the simulation, a distribution grid on low voltage level (400 V in Germany) with approx. 3100 residential consumers with approx. 3600 EVs is evaluated. The number of consumers is distributed over ten sub grids. The smallest grid has approx. 180 residential consumers, the largest grid approx. 480 residential consumers. The analyzed grid topology is shown in Figure 2. In the 100% PV-Scenario, the total amount of installed photovoltaic capacity is approx. 4.5 MW.

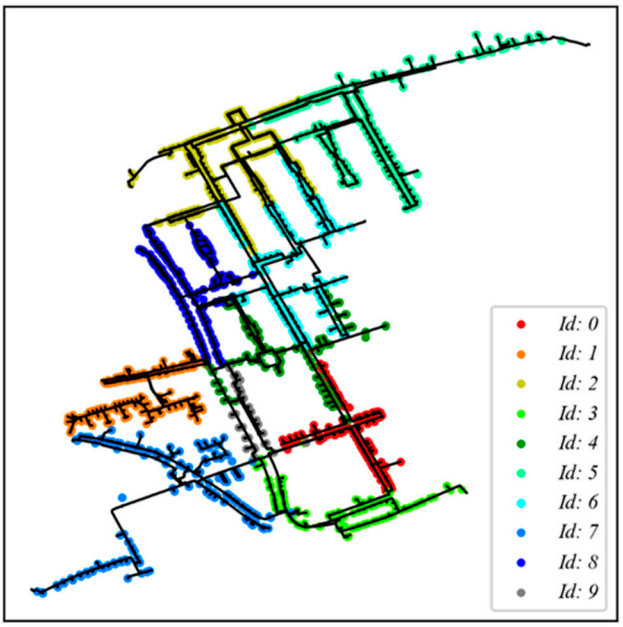

Figure 2. Investigated low-voltage (400 V) grid with 10 subgrids and 3100 consumers. The lines are colored according to the belonging subgrid ID.

The agent of the Flexibility Provider takes over the communication with the Capacity Provider for the consumers. The agent offers different tariffs depending on the analyzed scenario. The varying price signal in *Case B* and *C* is a composition of the price of the wholesale market (the day-ahead and continuous intraday market). Here, the wholesale market prices are based on the merit order principle and therefore take the scarcity of fluctuating renewable energy into account.

To summarize, the Flexibility Provider takes the role of the energy supplier and is responsible for energy purchase at the wholesale market. In the simulation framework, the agent only aggregates the generation and consumption time series and acts as an intermediary.

3.3. Consumer Behavior

In the simulation framework, three consumer types are implemented. To model the demand time series of each consumer, a SLP is used. Businesses and residential consumers with less than 100,000 kWh per year are forecasted and settled with such a SLP in Germany [37]. Bigger consumers, as the industry sector, are settled using historic meter values. Since no meter values are available for the industry consumers in the analyzed grid, a SLP for industry consumers is derived.

For this purpose, the total demand of residential and commercial customers was subtracted from the time series of the total load in Germany. Next, typical days are summarized. Therefore, all working days (Monday to Friday) are averaged for the annual seasons spring, summer, autumn, and winter. The same applies to Saturdays and Sundays. Therefore, twelve typical profiles are derived in hourly resolution for industry consumers. To estimate the annual consumption in the residential sector per hour, the SLP type H0 is used [37]. The profile is scaled with the total demand of 128 TWh/a. The same applies to commercial consumers, but with profile type G0 [37] and a yearly consumption of 135 TWh/a.

To summarize, all three consumer types are modeled with a SLP. For all residential areas, the H0 profile; for all businesses, the G0 profile; and for all bigger consumers, the derived profile (I0-Profile) is used.

In addition to the static demand, each household is represented by a Consumer-Agent, who has the objective to charge the EV with a specific strategy. The charging process always takes place at home.

To get a well-estimated charging demand, the mobility behavior of a single resident is modelled. The mobility behavior results from a statistic evaluation of the study "Mobilität in Deutschland" [36], where 154,420 households are surveyed. Based on these mobility statistics, different mobility events M_i are implemented. Each mobility event M_i belongs to one of the three categories work, errands, or hobby. A similar classification is carried out in [38]. To define a mobility event M_i, the following variables are used:

- $Ts_{t,j}$ as the start time at the destination in [HH:MM],
- $Td_{t,j}$ as the event duration in [min],
- $T_{t,j}$ as the travel time to the destination and/or back in [min],
- the absence time $Ta_{t,j}$ in [min] and
- $D_{t,j}$ as the distance between the home and destination in [km] for a day t.

To estimate the number of drivers and cars in the supply area, a mean consumption of 1500 kWh per year per person is assumed. With the data of the yearly energy consumption of each residential area, the number of persons per household is calculated and limited to two possible drivers. Each driver has his own EV. The mobility pattern of each driver is drawn as follows:

1. Draw the employment status and the relationship full-time or part-time. $Ta_{t,work}$ is 525 and 240 min for full- and part-time jobs.
2. Determine the mobility weekday $t \in DoW$, five days are drawn for work.
3. Terminate the start time $Ts_{t,j}$ depending on weekdays or weekend.
4. Get the one-way distance $D_{t,j}$.
5. Depending on the distance, determine the travel time $T_{t,j}$ and the means of transport.
6. Repeat step 2–5 for two hobbies with an absence time $Ta_{t,hobby}$ of 90 min and a certain number of errands with an absence time $Ta_{t,errand}$ of 35 min per week.

The maximum number of events is three per day, covering all categories. Next, drivers get a random EV. The vehicle must have at least the range to cover the maximum distance without charging. Equation (16) summarizes the condition for the range D_{EV}.

$$D_{EV} \geq 2 \max_{t \in T} \left(\sum_{j=1}^{N} D_{t,j} \right) \tag{16}$$

A random draw is made from all possible vehicles. The probability that a vehicle is drawn corresponds to the current registration statistics of the Federal Motor Transport Authority in Germany [2] The manufacturer's specification of the battery capacity E_{car}, the charging power P_{car}, and the consumption $EDem_{car}$ are used. The power P_{car} refers to a charging process at an Alternating Current (AC) charging station.

The potential of photovoltaics in the grid area was estimated using the data from source [39]. The portal offers the possibility to query PV data on a building-specific basis. The data include the roof areas of a building with azimuth, tilt, and maximum possible power at an efficiency of 17%. The data were prepared according to the known consumers in the supply area, so that each consumer receives at least one PV system in a 100% scenario. For multi-family houses, the total PV capacity of the building must be distributed among several consumers. The capacity was distributed to the individual residents in proportion to the total annual energy consumption of all consumers in the building.

The weather data from source [40] was used to calculate the final PV generation. The source provides weather data in a square grid of 0.25 degrees in hourly resolution

for the whole of Europe. For simplification, the weather data in the investigated supply area were averaged so that every consumer receives the same weather at every hour. The transfer of the weather data into a generation time series is done in Python with the library PVLib [41]. PV feed-in into the public grid is not considered. This means that there are no grid congestion situations due to too high PV feed-in.

Nevertheless, it is possible to quantify the effects of PV on the increasing grid utilization due to e-mobility. To investigate this, different consumer strategies were derived.

In the scenario cases, *Base Case*, *Case A*, and *Case B*, it was assumed that demand for electricity is independent of the dynamic retail price up to a defined threshold C_{Max}. When the threshold is exceeded, the result is a complete demand displacement for the electricity purchase of the EVs. On one hand, this leads to the desired guarantee that not many grid congestions occur. On the other hand, this modeling of the dynamic incentive effect is a clear abstraction of the actual relationship between demand (effect) and retail price (cause). In addition, this modeling technique results in a step function since demand evolves discontinuously at the threshold.

In classical microeconomics, demand is assumed to have a defined price elasticity, which can also reflect the real decision behavior of consumers more realistically. The assumption of an elasticity is also of great importance for the analysis of incentive models for load control, e.g., market- and grid-serving charging [42]. Therefore, a set of price elasticity functions is used in scenario *Case C*.

For the derivation the price elasticity, survey results were used for this study, which were presented in detail in [43]. In the survey design, approximately 90 participants were asked to define three price levels according to the following questions, among others, as part of the online survey: The study provided the following information on price and charging behavior:

- The following total price C_{Min} at AC charging stations is low for me—I would try to charge (Stated in ct/kWh).
- The following total price C_{Max} at AC charging stations is too high for me—I would not charge (Stated in ct/kWh).
- The following total price *PLimit* at AC charging stations is quite high for me—but I would charge if necessary (Stated in ct/kWh).

Figure 3 shows the results for C_{Min} and C_{Max} of the survey in a scatter histogram. Above and to the right of the scatter plot, the absolute frequency distribution (histograms) of C_{Min} and C_{Max} are also plotted. The scatterplot indicates a correlation between C_{Max} and C_{Min}. A higher indication of C_{Min} tends to result in feedback of an increased C_{Max} for the same respondent. This correlation will be analyzed in more detail using a subsequent regression analysis.

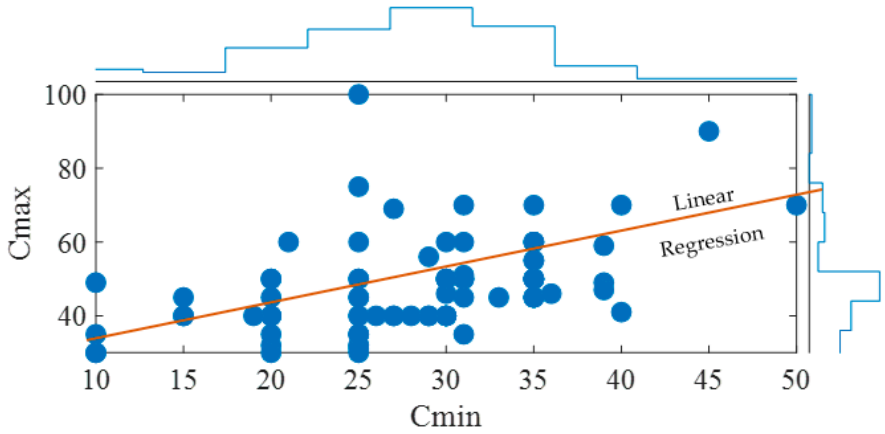

Figure 3. Distribution and correlation between the price levels C_{Min} and C_{Max} in [ct/kWh].

What is striking in the histogram for C_{Min} is the broad distribution of responses. This suggests that end consumers have different price sensitivities, because all customers got the same average price level of 40 ct/kWh in the survey.

In the following, C_{Min} and C_{Max} are to be interpreted as marginal prices at a very high and low SoC. In a next step, the relationship between C_{Min} and C_{Max} is quantified using linear regression and the significance of the slope parameter is assessed. The estimator for the slope parameter m in the amount of 0.75 is significant compared to the H0 hypothesis $m = 0$. The slope of the function between the point C_{Limit} is derived from the difference of the two marginal prices C_{Min} and C_{Max} to the marginal price C_{Limit}. The results of the subsequent regression analysis are shown in Table 2.

Table 2. Regression parameters of price sensitivity curve.

C_{Min} to C_{Max}	Estimate	SE	*p*-Value
Intercept	26.75	4.71	1.94×10^{-7}
m	0.75	0.16	1.31×10^{-5}
C_{Min} to $C_{Limit} - C_{Min}$			
Intercept	26.73	4.70	1.95×10^{-7}
m	−0.25	0.16	0.12
C_{Max} to $C_{Max} - C_{Limit}$			
Intercept	−5.36	1.75	0.003
m	0.27	0.035	2.65×10^{-11}

A positive correlation between the difference of C_{Min} and C_{Max} to C_{Limit} could also be demonstrated, indicating a differentiation of the slopes of the demand functions.

For the concrete demand function, a simplified assumption was made that the points C_{Max}, C_{Limit} and C_{Min} are associated with a respective SoC of 20%, 40% and 90%. The values 90% and 20% correspond to a battery-saving charging behavior. [N6] The third interpolation point of 40% was derived from the fact that at a SOC of 40%, over 90% of all motion profiles can be mapped.

From the regression analysis, the support points for the continuous demand function F(SoC) were derived: $C_{Max} = (C_{Max}; 15\%)$, $C_{Limit} = (C_{Max} - 0.27 \cdot C_{Max}; 40\%)$, $C_{Min} = (C_{Min}; 85\%)$. The H0-Hypthesis for the slope between min and $C_{Max} - C_{Min}$ is rejected in case of $\alpha < 12\%$. The lower value of m underlines the existence of a different slope along the curve, but a future survey with a larger number of participants should be conducted to further investigate the relationship and decrease the standard deviation of the estimator. The course of the demand function between the grid points was interpolated with the help of a spline. In a final step, it was considered that, according to the survey results, individual demand curves can be assumed (see histogram of C_{Min} in Figure 3). This is particularly important when considering the simultaneity of the reaction to a price change.

Based on the survey results, it can be expected that a defined price signal results in a demand-specific reduction in demand. In terms of content, this reflects a different and individual "range anxiety" of individual residents, since the demand restraint leads to a reduced SoC. Residents will judge the "value" of the SoC differently.

The graph in Figure 4 shows thirteen exemplary trajectories of each demand function F(SoC). Each curve represents a corresponding risk preference. This becomes comprehensible when considering a defined end customer price with the associated advised SoC. For example, at a price of approx. 62 ct/kWh, a very risk-averse household will achieve a minimum SoC of about 30%, while a very price-sensitive household will not seek charging at this price and will charge its EV solely from its home PV system. Conversely, when the retail price is below the median price level of 40 ct/kWh, the individual profiles also aim for a different SoC state. This corresponds to the fact that price-sensitive users want to maintain charging flexibility for their own PV electricity or for future hours with even significantly lower electricity prices and thus do not aim for a SoC of 100%.

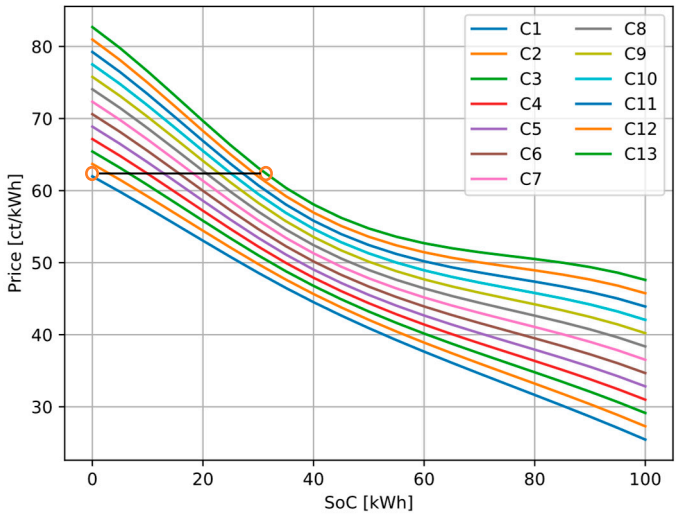

Figure 4. 13 Trajectories of each demand function depending on the State of charge—drawn from the survey. The trajectories show different exemplary price sensitivity behavior.

The assignment of end users to one of the mapped demand functions F(SoC) is done with a random variable that picks up the relative frequency distribution of C_{Min}. This ensures that extreme manifestations of risk aversion occur less frequently in the total consumer base than demand functions located in the middle of the set of curves.

Exemplary behavior curves of a specific car are shown in Figure 5. The usage behavior is the same through all scenarios since the visited car stays the same. In the *Base Case*, the car is only charged when it becomes available without optimizing, using most of the energy from the grid. The second Case shows how optimizing the PV usage increases the SoC and reduces charging from the grid. As the market price is constant, the grid charging is optimized according to the grid fee signal, resulting in many short charging periods. In *Case B*, a dynamic spot market price is added, which has a much larger impact than the grid fee did, resulting in a preference to charge when the market prices are low. Often, market prices are low during the day when cars are unavailable (see Figure 6), creating a preference to charge shortly before or after the unavailability of the car. Finally, *Case C* introduces the derived demand function F(SoC), which is based on the current SoC and results in a lower average SoC.

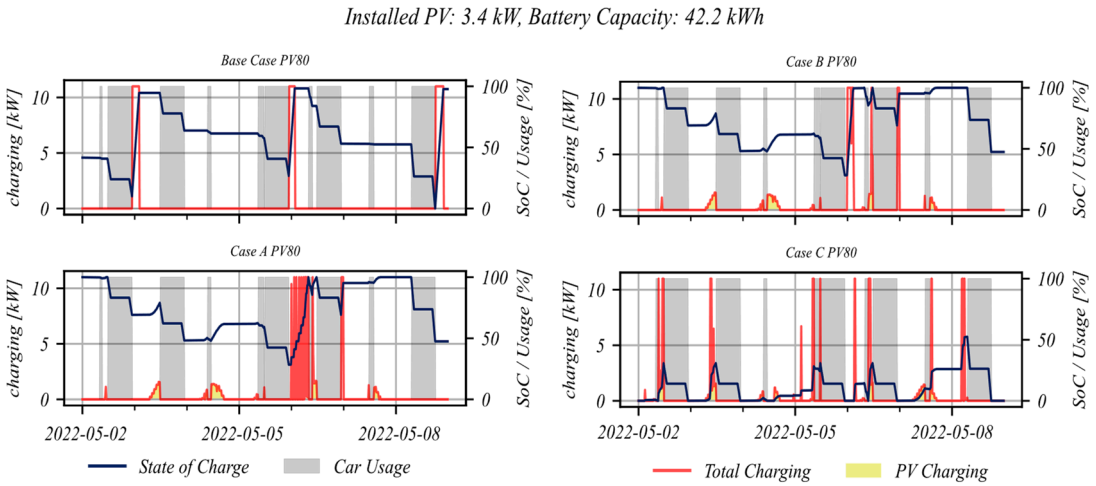

Figure 5. Exemplary resulting charging curves of the same EV visualized for the *Base Case*, *Case A*, *Case B*, and *Case C* with 80% installed PV potential on buildings in the simulation.

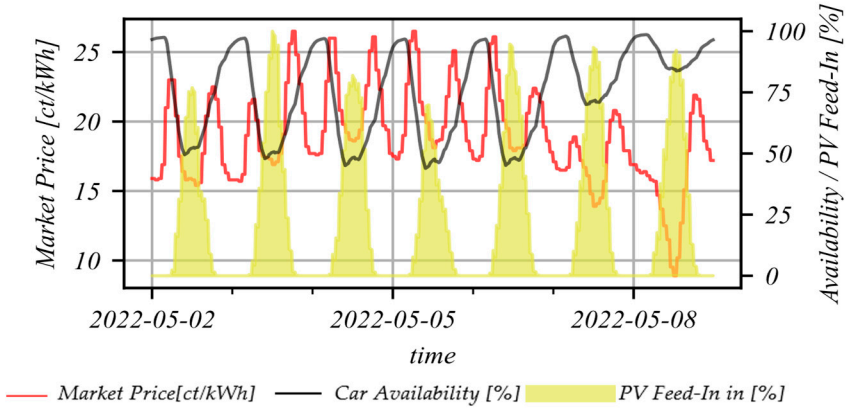

Figure 6. Spot market prices + percentage of PV feed-in in contrast to the car availability.

4. Results

In this section, the main results of the evaluation are presented. For this purpose, the analyses are divided into a comparison of the *Base Case* with *Case A* (increase of PV self-consumption) and an analysis of the strategies regarding a more realistic representation of user behavior in the case of dynamic market prices (*Case B* and *Case C*).

For the following explanations, it is useful to remember Figure 6. It shows the market price, the normalized PV-feed in, and the average availability of the EVs at home. The figure illustrates the challenge of synchronizing the charging of EVs with periods of low prices or high PV feed-in in the different use cases. Times of high PV-feed in and low market prices are often attended to low availability of EVs for charging operations.

4.1. Analysis of a Self-Supply-Based Charging Strategy

In a first step of the analysis, it is analyzed whether an increased PV self-consumption can significantly contribute to the reduction of the grid load. Figure 7 shows the sorted duration line of the average transformer utilization. In all simulations of different PV capacities in *Case A*, an average transformer utilization of >50% is observed in less than 2% of the simulation hours. An increase in installed PV capacity results in a more noticeable reduction in average utilization, especially in the middle and at the right edge of the duration line.

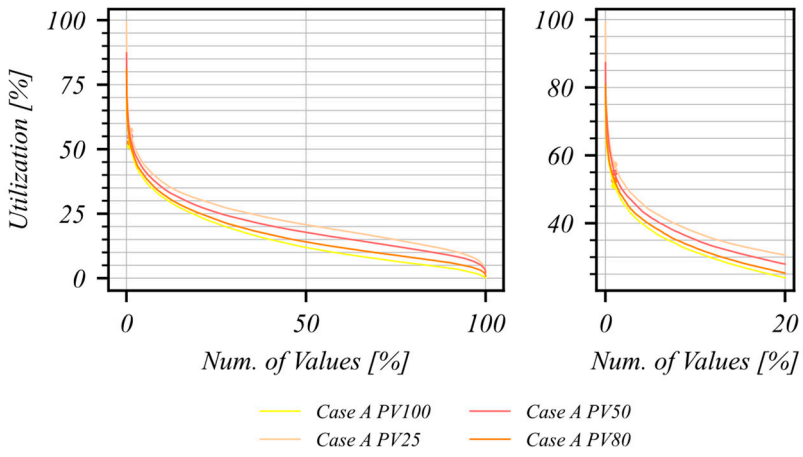

Figure 7. Impact of the PV expansion on the main transformer utilization.

When considering the 1% quantile, which shows an average utilization between 50–55%, the reduction effect is less noticeable with an increase in installed PV capacity. This effect is understandable since the PV feed-in is based on a fluctuating supply (solar radiation) and thus cannot be controlled, and in addition, there is a natural asynchrony

between PV feed-in and charging demand (see Figure 6). A closer look at the values in the 1% quantile shows that these occur in hours with low/no solar radiation where the PV supply cannot act grid serving.

A more detailed breakdown of the utilization analysis for the respective 10 transformers of the distribution grid shows that the PV effect is also differentiated depending on the area. The type of use in the respective area, and thus the ratio of installed PV capacity to the number of EVs, have a decisive influence on the reduction potential. The upper graph of Figure 8 shows the number of EVs and the potential of PV generation. Basically, a correlation with the transformer utilization is shown here in the second graph. The different reduction potential of the second graph can be explained in connection with the different shares of PV to electromobility in the individual areas. Therefore, the most significant impact can be seen in subgrid 2. Figure 8 shows that a detailed evaluation is useful, especially for inhomogeneous grid areas, to determine the influence of different PV-installed capacity precisely.

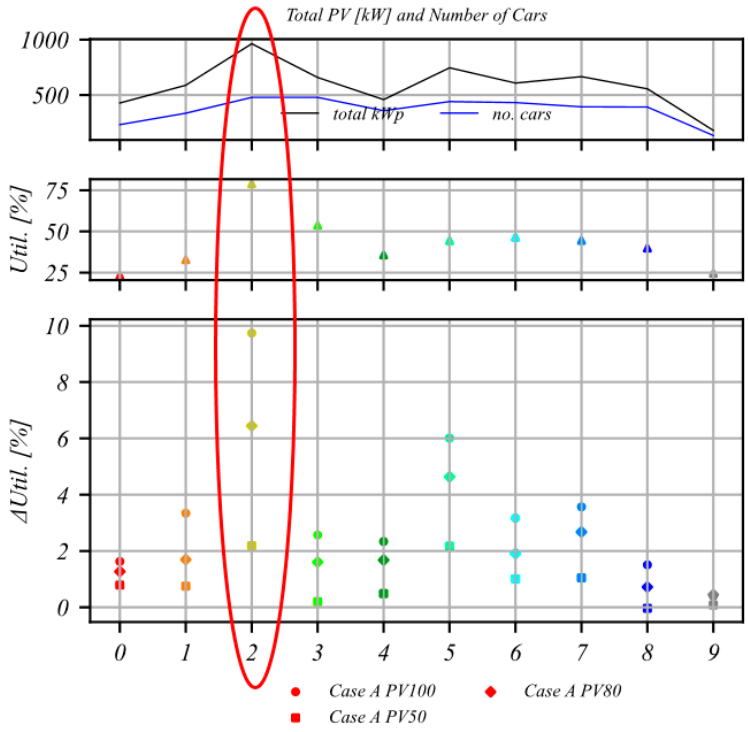

Figure 8. Impact of the demand function on the utilization on grid level for all 10 transformers (0–9 and colored) with its PV installation size and number of cars in its subgrid.

4.2. Analysis of More Complex Derivation of the Charging Behavior

In the following, the effects of the more realistic mapping of the demand function F(SoC) and the consideration of a dynamic market price on the grid utilization are evaluated. The individual utilization under a high penetration of installed PV capacity of 80% of the potential is shown in the right panel of Figure 9. The 1% quantile as a risk measure for the grid utilization is clearly differentiated over the four considered cases. It is understandable that the introduction of a self-consumption optimizing (red) and additionally to a dynamic market price aligned charging behavior (green) lead to a clear increase in the utilization factor in the 1% quantile. However, from the authors' point of view, a grid planning based on these values would lead to an inefficient grid planning. This is shown by the scenario of an additional consideration of a differentiated demand elasticity (red) that is closer to reality. The higher simultaneity in the charging behavior caused by the dynamic market price component does not represent individual risk preferences—but creates a swing effect for all simulation households. The demand functions parameterized based on the survey mitigate

this effect of the dynamic market price component in the residential tariff. This result demonstrates the need for a more in-depth analysis of user behavior in further research to map this aspect more precisely and to refine the impact analysis on grid utilization.

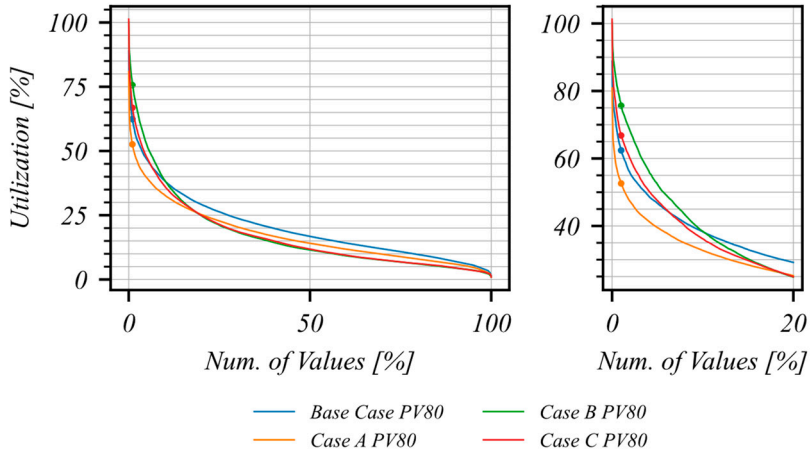

Figure 9. Impact of the demand function on the mean transformer utilization.

4.3. Grid and Economic Impact Analyses

In the following analyses, the grid utilization as well as the economic implications of the individual cases are considered from the end customer's perspective.

The individual cases require a corresponding regulatory framework. It is of decisive importance to know about the individual benefit function of the user's behavior. Assuming an economically rational agent, the more complex user behavior depicted in *Case C* should therefore be compatible with an associated economic incentive.

In Table 3, the consumption (grid- and PV-side) as well as the associated costs for a detailed analysis (split market- and grid-side) are presented.

Table 3. Result overview for the scenarios with a used PV potential of 80%.

	Unit	***Base Case***	***Case A***	***Case B***	***Case C***
Charging					
Grid	%	98	71	71	69
PV	%	2	29	29	31
Shifted	%	<0.3	<0.1	4.9	38.9
Pricing					
Average Cost	ct/kWh	21.8	15.6	15.2	14.0
Market	%	78	79	72	73
Grid	%	22	21	28	27
ø Grid Fee	ct/kWh	4.3	3.9	3.4	3.0
95% quantile	ct/kWh	6.4	5.8	7.4	6.6
ø 95–100%	ct/kWh	6.8	6.2	8.8	7.5
Utilization					
ø Util.	%	20	17	17	17
95%-quantile	%	47	40	52	47
ø 95–100%	%	56	47	67	59

Figure 10 shows the utilization for a given transformer throughout all scenarios for one week of simulation time. Comparing the *Base Case* to *Case A*, one can see that a reduction in grid utilization is performed through the optimization of the PV charging. Furthermore, adding the price signal without differentiation in the user behavior creates large utilization spikes (*Case B*), which are reduced if the benefit function F(SoC) is added (*Case C*).

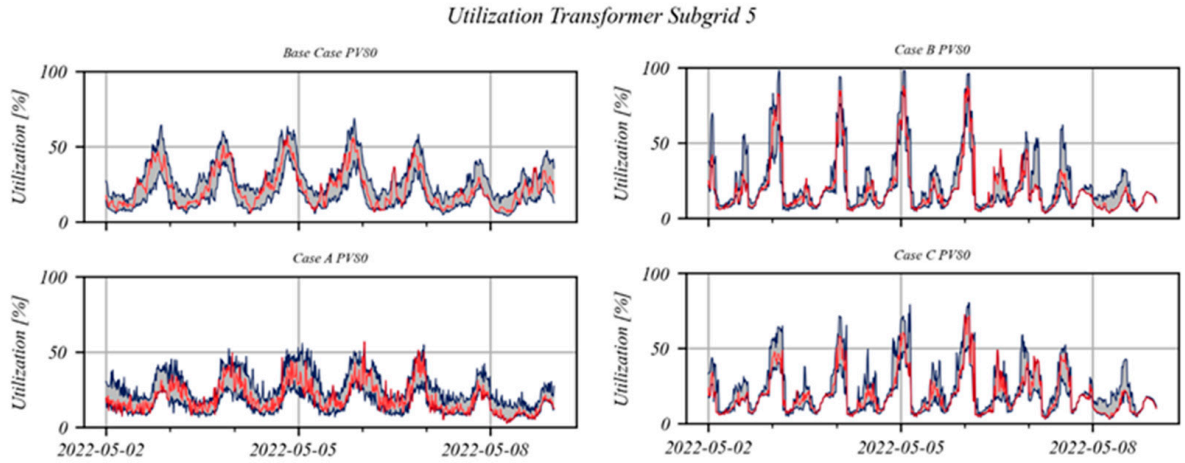

Figure 10. Utilization in percent on an exemplary subgrid throughout the different scenarios analyzed in this paper—the minimum, mean, and maximum utilization of the given transformer are shown as lower and upper band of this.

On one hand, looking at consumption shows the increase in PV self-consumption in *Case A–C* described earlier. The largest cost reduction is achieved by the significant increase in PV self-consumption from *Case A* onwards due to better synchronization of charging and PV feed-in.

The further cost reduction in *Case B* and *Case C* is largely based on an additional response to the dynamic price signal. It is noticeable that the differentiation of the demand function can significantly reduce the peak grid congestions as also seen in Figure 9. The level in this range almost reaches the utilization level of the *Base Case* again (without dynamic market price signal). However, this must be contrasted with the fact that a correspondingly mapped user behavior, in contrast to PV synchronization, is only provided with a relatively low economic incentive in the model evaluation (reduction of the market-side costs from 15.2 to 14.0 ct/kWh).

Optimizing PV usage reduces the cost by 6.2 ct/kWh, which shows the greatest potential for cost reduction from the users' point of view.

5. Conclusions

In this paper, we presented a multi-agent-based simulation for a realistic view of possible grid congestions due to the increase in e-mobility. This model is open-source available on GitHub at https://github.com/NOWUM/smartdso/. Furthermore, we investigated the effect of dynamic grid and market prices. To summarize, the dynamic market prices result in high simultaneity factors, which can be handled by the provided dynamic grid fee and differentiated price sensitivity curves.

In the future, it can be assumed that due to increased fluctuating feed-in, the day-ahead and intraday prices will be subject to higher fluctuations, and thus, the incentive for dynamic tariffs should increase. Nevertheless, it can be assumed that a very high degree of automation and a low restriction of the quality of life are required to observe the user behavior depicted here in practice.

The presented methodology focuses on the agent-based modeling of individual mobility behavior where each mobility demand is priced by the grid operator/capacity provider.

Modeling the user's behavior independently of the grid operator prices allows simulating heterogenous individual charging behavior of the agents.

The assigned user behavior in *Case C* leads to a significant change in grid utilization, which highlights the requirement for more realistic modelling of charging behavior when analyzing future grid development plans. As a next step, the user behavior and scope of functions of the market actors should be improved. Moreover, other sector-coupled

technologies such as power-to-heat and battery storages should be introduced to cover the total scope of energy demand. This allows to further investigate a more realistic view of the impact of flexibility from e-Mobility and PV systems on the energy system.

Author Contributions: Conceptualization, F.M., C.R., R.S. and D.S.; methodology, R.S., F.M. and C.R.; software, F.M. and C.R.; validation, F.M., C.R. and R.S.; formal analysis, R.S. and C.R.; investigation, F.M. and C.R.; resources, D.S.; data curation, F.M. and C.R..; writing—original draft preparation, F.M., C.R., R.S. and D.S.; writing—review and editing, F.M., C.R., R.S. and D.S.; visualization, C.R. and R.S.; supervision, R.S.; project administration, D.S.; funding acquisition, D.S. All authors have read and agreed to the published version of the manuscript.

Funding: This research was partially financed by the European Fund for Regional Development (EFRE), Grant Nr. EFRE-0801805.

Data Availability Statement: Results can be reproduced using the open-source software provided. Unfortunately, we do not have permission to publish the grid data to the public as it was only made available for research.

Conflicts of Interest: The authors declare no conflict of interest. The funders had no role in the design of the study; in the collection, analyses, or interpretation of data; in the writing of the manuscript; or in the decision to publish the results.

Nomenclature

RES	Renewable energy sources
EEG	Erneuerbare-Energien-Gesetz
EV	Electric Vehicle
PV	Photovoltaic
PSA	Power System Analysis
SLP	Standard Load Profile
AC	Alternating Current
SoC	State of Charge
T	Set of time steps
t	time step
C	Set of EV/cars
c	car
D	[km] Travel Distance
D_{EV}	[km] range of the EV
P_{car}	[kW] maximum charging power of a car
E_{car}	[kWh] maximum capacity of a car
$EDem_{car,t}$	[kW] demand of a car at time step t
$V_{car,t}$	[kWh] capacity level of a car at time step t
G_t	[ct/kWh] dynamic grid fee at time step t
B	benefit, which depends on $V_{car,t}$
S	set of segments
s	segment of linearized B function
z_s	variable to indicate the active segment
$SegVLow_s$	lower capacity of linearized B function
$SegVUp_s$	upper capacity of linearized B function
$SegCoef_s$	slope of the linearized B function
$VTotal$	[kWh] sum of single $V_{car,t}$
Ppv_t	[kW] power of the attached PV system at t
$PCharge_t$	[kW] charged power at timestep t
C_{Limit}	[ct/kWh] mean price for SoC 40%
C_{Max}	[ct/kWh] upper price, charge when SoC < 20%
C_{Min}	[ct/kWh] lower price, charge when SoC < 90%

References

1. Arbeitsgruppe Energie-Monitoring. *Monitoringbericht 2021*; Bundesnetzagentur für Elektrizität, Gas, Telekommunikation, Post und Eisenbahnen: Berlin, Germany, 2021; p. 540.
2. Statistik Kraftfahrtbundesamt. Available online: https://www.kba.de/DE/Statistik/Fahrzeuge/fahrzeuge_node.html;jsessionid=6437EAC3E3F71138982F44CD869FEFEC.live21324 (accessed on 27 October 2022).
3. Elektromobilität in Deutschland. Available online: https://www.bmwk.de/Redaktion/DE/Dossier/elektromobilitaet.html415 (accessed on 3 April 2023).
4. Robinson, J.; Erickson, L.E. Infrastructure for Charging Electric Vehicles. In *Solar Powered Charging Infrastructure for Electric Vehicles*; Erickson, L.E., Robinson, J., Brase, G., Cutsor, J., Eds.; CRC Press: Boca Raton, FL, USA, 2016; pp. 35–51. ISBN 978-1-4987-3156-0.
5. Kasten, P.; Minnich, L.; Randrianarisoa, J.; Ritter, D.; Vogel, M.; Dünzen, K.; Just, L.; Novirdoust, A.A.; Diers, H.; Niesler, N.; et al. Szenarien Und Regulatorische Herausforderungen Für Den Aufbau Der Ladeinfrastruktur Für Elektrische Pkw Und Lkw. Available online: https://www.oeko.de/fileadmin/oekodoc/ENSURE-II_Ladeinfrastruktur.pdf (accessed on 3 April 2023).
6. Lopes, J.A.P.; Soares, F.J.; Almeida, P.M.R. Integration of Electric Vehicles in the Electric Power System. *Proc. IEEE* **2011**, *99*, 168–183. [CrossRef]
7. Green, R.C.; Wang, L.; Alam, M. The Impact of Plug-in Hybrid Electric Vehicles on Distribution Networks: A Review and Outlook. *Renew. Sustain. Energy Rev.* **2011**, *15*, 544–553. [CrossRef]
8. Brinkel, N.; Alskaif, T.; van Sark, W. The Impact of Transitioning to Shared Electric Vehicles on Grid Congestion and Management. In Proceedings of the 2020 International Conference on Smart Energy Systems and Technologies (SEST), Istanbul, Turkey, 7–9 September 2020.
9. Resch, M.; Buhler, J.; Schachler, B.; Sumper, A. Techno-Economic Assessment of Flexibility Options Versus Grid Expansion in Distribution Grids. *IEEE Trans. Power Syst.* **2021**, *36*, 3830–3839. [CrossRef]
10. Brinkel, N.B.G.; Schram, W.L.; AlSkaif, T.A.; Lampropoulos, I.; van Sark, W.G.J.H.M. Should We Reinforce the Grid? Cost and Emission Optimization of Electric Vehicle Charging under Different Transformer Limits. *Appl. Energy* **2020**, *276*, 115285. [CrossRef]
11. Zethmayr, J.; Kolata, D. Charge for Less: An Analysis of Hourly Electricity Pricing for Electric Vehicles. *World Electr. Veh. J.* **2019**, *10*, 6. [CrossRef]
12. Sinha, S.; Chandel, S.S. Review of Software Tools for Hybrid Renewable Energy Systems. *Renew. Sustain. Energy Rev.* **2014**, *32*, 192–205. [CrossRef]
13. Gottwalt, S. Managing Flexible Loads in Residential Areas. 2015. Available online: https://publikationen.bibliothek.kit.edu/1000048803 (accessed on 3 April 2023).
14. Su, J. Smart Management of Electric Vehicles Charging in Distribution Networks. Ph.D. Thesis, Auckland University of Technology, Auckland, New Zealand, 2020.
15. Babrowski, S.; Heinrichs, H.; Jochem, P.; Fichtner, W. Load Shift Potential of Electric Vehicles in Europe. *J. Power Sources* **2014**, *255*, 283–293. [CrossRef]
16. Su, W.; Wang, J.; Roh, J. Stochastic Energy Scheduling in Microgrids With Intermittent Renewable Energy Resources. *IEEE Trans. Smart Grid* **2014**, *5*, 1876–1883. [CrossRef]
17. Diaz-Cachinero, P.; Munoz-Hernandez, J.I.; Contreras, J. A Linear Model for Operating Microgrids with Renewable Resources, Battery Degradation Costs and Electric Vehicles. In Proceedings of the 2018 15th International Conference on the European Energy Market (EEM), Lodz, Poland, 27–29 June 2018; IEEE: Lodz, Poland, 2018; pp. 1–5.
18. Soares, J.; Borges, N.; Fotouhi Ghazvini, M.A.; Vale, Z.; de Moura Oliveira, P.B. Scenario Generation for Electric Vehicles' Uncertain Behavior in a Smart City Environment. *Energy* **2016**, *111*, 664–675. [CrossRef]
19. Schäuble, J.; Kaschub, T.; Ensslen, A.; Jochem, P.; Fichtner, W. Generating Electric Vehicle Load Profiles from Empirical Data of Three EV Fleets in Southwest Germany. *J. Clean. Prod.* **2017**, *150*, 253–266. [CrossRef]
20. Pflaum, P.; Alamir, M.; Lamoudi, M.Y. Probabilistic Energy Management Strategy for EV Charging Stations Using Randomized Algorithms. *IEEE Trans. Contr. Syst. Technol.* **2018**, *26*, 1099–1106. [CrossRef]
21. Gerritsma, M.K.; AlSkaif, T.A.; Fidder, H.A.; Sark, W.G.J.H.M. van Flexibility of Electric Vehicle Demand: Analysis of Measured Charging Data and Simulation for the Future. *WEVJ* **2019**, *10*, 14. [CrossRef]
22. Wang, B.; Zhao, D.; Dehghanian, P.; Tian, Y.; Hong, T. Aggregated Electric Vehicle Load Modeling in Large-Scale Electric Power Systems. *IEEE Trans. Ind. Applicat.* **2020**, *56*, 5796–5810. [CrossRef]
23. Diaz-Cachinero, P.; Munoz-Hernandez, J.I.; Contreras, J. A Microgrid Model With EV Demand Uncertainty and Detailed Operation of Storage Systems. *IEEE Trans. Ind. Applicat.* **2022**, *58*, 2497–2511. [CrossRef]
24. Xydas, E.; Marmaras, C.; Cipcigan, L.M. A Multi-Agent Based Scheduling Algorithm for Adaptive Electric Vehicles Charging. *Appl. Energy* **2016**, *177*, 354–365. [CrossRef]
25. Zhang, J.; Yan, J.; Liu, Y.; Zhang, H.; Lv, G. Daily Electric Vehicle Charging Load Profiles Considering Demographics of Vehicle Users. *Appl. Energy* **2020**, *274*, 115063. [CrossRef]
26. Karapidakis, E.; Tsikalakis, A.; Paspatis, A.; Fotakis, E.; Stavrakakis, G.; Chatzipoulka, C.; Zervas, P. Grid Operation Assessment under a Specific EV Chargers Deployment Plan in the City of Heraklion. *Electronics* **2021**, *10*, 2831. [CrossRef]
27. Konstantinidis, G.; Karapidakis, E.; Paspatis, A. Mitigating the Impact of an Official PEV Charger Deployment Plan on an Urban Grid. *Energies* **2022**, *15*, 1321. [CrossRef]

28. Paspatis, A.; Fiorentzis, K.; Katsigiannis, Y.; Karapidakis, E. Smart Campus Microgrids towards a Sustainable Energy Transition—The Case Study of the Hellenic Mediterranean University in Crete. *Mathematics* **2022**, *10*, 1065. [CrossRef]
29. Pagani, M.; Korosec, W.; Chokani, N.; Abhari, R.S. User Behaviour and Electric Vehicle Charging Infrastructure: An Agent-Based Model Assessment. *Appl. Energy* **2019**, *254*, 113680. [CrossRef]
30. Sundstrom, O.; Binding, C. Flexible Charging Optimization for Electric Vehicles Considering Distribution Grid Constraints. *IEEE Trans. Smart Grid* **2012**, *3*, 26–37. [CrossRef]
31. Sundström, O.; Binding, C. Planning Electric-Drive Vehicle Charging under Constrained Grid Conditions. In Proceedings of the 2010 International Conference on Power System Technology, Hangzhou, China, 24–28 October 2010; pp. 1–6.
32. Sun, L.; Lubkeman, D. Agent-Based Modeling of Feeder-Level Electric Vehicle Diffusion for Distribution Planning. *IEEE Trans. Smart Grid* **2021**, *12*, 751–760. [CrossRef]
33. Vopava, J.; Bergmann, U.; Kienberger, T. Synergies between E-Mobility and Photovoltaic Potentials—A Case Study on an Urban Medium Voltage Grid. *Energies* **2020**, *13*, 3795. [CrossRef]
34. Tsiakis, P.; Shah, N.; Pantelides, C.C. Design of Multi-Echelon Supply Chain Networks under Demand Uncertainty. *Ind. Eng. Chem. Res.* **2001**, *40*, 3585–3604. [CrossRef]
35. Brown, T.; Hörsch, J.; Schlachtberger, D. PyPSA: Python for Power System Analysis. *JORS* **2018**, *6*, 4. [CrossRef]
36. infas, DLR, IVT und infas 360 Mobilität in Deutschland (on behalf of BMVI). 2018. Available online: https://www.mobilitaet-in-deutschland.de/archive/pdf/MiD2017_Ergebnisbericht.pdf (accessed on 10 April 2023).
37. Standardlastprofile-Strom. Available online: https://www.bdew.de/energie/standardlastprofile-strom/ (accessed on 27 October 2022).
38. Jazaeri, J.; Gordon, R.L.; Alpcan, T. Influence of Building Envelopes, Climates, and Occupancy Patterns on Residential HVAC Demand. *J. Build. Eng.* **2019**, *22*, 33–47. [CrossRef]
39. Solarkataster. Available online: https://www.energiedaten.nrw.de (accessed on 27 October 2022).
40. Muñoz Sabater, J. ERA5-Land Hourly Data from 1950 to Present. Copernicus Climate Change Service (C3S) Climate Data Store (CDS). 2019. Available online: https://cds.climate.copernicus.eu/cdsapp#!/dataset/10.24381/cds.e2161bac?tab=overview (accessed on 10 April 2023).
41. Holmgren, F.; Hansen, W.; Mikofski, A. Pvlib Python: A Python Package for Modeling Solar Energy Systems. *JOSS* **2018**, *3*, 884. [CrossRef]
42. Frank, D.; Kleis, K.; Dr., Schmid, E.; Schrader, T.-S.; Schwarze, E. Hendrik Zimmermann Effektive Stromnetzentgelte Für Die Transformation. Available online: https://www.germanwatch.org/de/85071 (accessed on 3 April 2023).
43. Georg, J.H. "Smartes" Laden an Öffentlichen Ladesäulen: Anreizmodell Für Markt- Und Netzdienliches Laden, Energiewirtschaftliche Tagesfragen 72. 2022. Available online: http://www.jhc-energie.de/.cm4all/uproc.php/0/et-Artikel-29072022-PDF_18115_et_7-8_2022_S.37-41.pdf (accessed on 3 April 2023).